

CrossMark
click for updatesCite this: *RSC Adv.*, 2016, 6, 58541

An ultrasensitive aptasensor for chlorpyrifos based on ordered mesoporous carbon/ferrocene hybrid multiwalled carbon nanotubes

Yancui Jiao,^{ab} Huiying Jia,^{ab} Yemin Guo,^{*ab} Haiyun Zhang,^{ab} Zhiqiang Wang,^{ab} Xia Sun^{*ab} and Jing Zhao^a

In this study, we designed a novel and ultrasensitive aptamer sensor for the quantitative detection of chlorpyrifos. To improve the sensitivity of the aptasensor, mesoporous carbon (OMC) functionalized by chitosan (OMC-CS) and ferrocene hybrid chitosan (CS) dispersed multiwalled carbon nanotubes (Fc@MWCNTs-CS) were modified on the electrode surface. OMC-CS has a high specific surface area, high porosity and ideal dispersibility which was used to efficiently capture larger amounts of material. Fc@MWCNTs-CS can efficiently capture more aptamer and increase electron transfer between the work electrode surface and potassium ferricyanide due to the good biocompatibility and electrical conductivity. The fabrication of the aptasensor was characterized using cyclic voltammetry, scanning electron microscopy and energy dispersive spectrometry. Under optimal conditions the designed aptasensor exhibited a wide linear range from 1 to 10⁵ ng mL⁻¹ with a low detection limit of 0.33 ng mL⁻¹ (S/N = 3) for chlorpyrifos. The proposed chlorpyrifos aptasensor exhibited high selectivity, reproducibility and stability performance, which may open a new door for the ultrasensitive detection of chlorpyrifos residues in vegetables and fruits.

Received 24th March 2016

Accepted 1st June 2016

DOI: 10.1039/c6ra07735h

www.rsc.org/advances

1. Introduction

Chlorpyrifos (*O,O*-diethyl-*O*-3,5,6-trichloro-2-pyridylphosphorothioate, CPF) is an organophosphorus pesticide, which has a broad spectrum, efficient and moderate toxicity, a long residual effect period, and good stomach toxicity. It is mainly used for the prevention and control of harmful insects and mites on cotton, vegetables, tea, fruit and crops.¹ Moreover, it is one of the largest used tonnage pesticides in the international market.² The presence of pesticide residues in vegetables may pose a risk to human health due to the pesticides' potential toxicity.³ In some cases, it has been suggested that some diseases, such as acute neurological toxicity, neurodevelopmental impairment, cancer, allergies, neurological disorders and reproductive disorders, may be related to pesticide exposure.^{4–7}

To date, many analytical technologies have been developed for pesticide detection, such as high-performance liquid chromatography (HPLC),^{8–10} gas chromatography (GC).^{11,12} These instrument-based techniques have high sensitivity and low

detection limit, but they are expensive, tedious and require trained operators. ELISAs possess the advantages of rapidness and simplicity, while it is vulnerable to the interference from organic solvent or matrix components.¹³ Compared with these methods, electrochemical biosensors with advantages of fast response, high sensitivity, low cost, and on-site analysis, have been a promising alternative to rapidly detect pesticides.¹⁴ For instance, AChE electrochemical biosensors are particularly attractive due to their fast response and high sensitivity.^{15,16} But it can only be used to detect a class of pesticides. Immunosensor, with its high sensitivity and specificity, has been widely used to detect pesticide,¹⁷ viruses and bacteria,¹⁸ which based on antigen and antibody interaction.¹⁹ However, antibody is temperature sensitive and exhibits dissociation constant that is strongly influenced by the physiological condition.²⁰ Compared with antibodies and enzymes, aptamer-based biosensors have exceptional merits among various applications.²¹

Aptamers are RNA or DNA molecules with specific 3D structures. They can be selected through an *in vitro* selection process called systematic evolution of ligands by exponential enrichment (SELEX), and they are capable of recognizing and binding a variety of targets ranging from small molecules to organisms. Owing to their unique advantages of chemical recognition, accuracy, ease of modification, *in vitro* synthesis, high purity and stability, aptamers have been widely used in analysis applications.²² Moreover, due to their relative ease of tailored binding affinity, modification, isolation and storage,²³

^aSchool of Agriculture and Food Engineering, Shandong University of Technology, No. 12, Zhangzhou Road, Zibo 255049, Shandong Province, People's Republic of China. E-mail: sunxia2151@gmail.com; Fax: +86-533-2786558; Tel: +86-533-2786558

^bShandong Provincial Engineering Research Center of Vegetable Safety and Quality Traceability, No. 12, Zhangzhou Road, Zibo 255049, Shandong Province, People's Republic of China

aptamers exhibit several unprecedented advantages compared with antibodies.²⁴ Electrochemical aptasensor is a kind of biosensor which measuring the electrochemical signal changes before and after affinitive interactions between the aptamer and target. Until now, electrochemical aptasensors have been rapidly developed to detect different targets by combining various electrochemical techniques with aptamer-based signal conversion strategies.²⁵ Especially, label-free electrochemical aptasensors play an important role due to their simplicity, convenience, and low cost.²⁶ Recently, a label-free DNA aptasensor based on loop-mediated isothermal amplification has been reported for the detection of ochratoxin A.²⁷ While the aptasensor used for pesticide detection has been still less reported.

In recent years, various carbon nanomaterials have been widely employed to improve the performance of electrode. The ordered mesoporous carbons (OMCs) are one type of new advanced carbon materials, initially synthesized in 1999.²⁸ Ever since, the OMCs have been the matter of concern due to their unique properties such as high specific surface area, ordered mesostructure, tunable pore size, low density, high conductivity, chemical stability, and biocompatibility.²⁹ OMC can be used as building blocks in hybrid materials, and provides an excellent platform and microenvironment for immobilized biomolecules such as DNA, enzyme and protein.³⁰ Accordingly, the existing report³¹ provides strong evidence that OMC could be acted as an effective candidate for fabricating new type of electrochemical sensors and biosensors. However, OMC lacks enough film forming ability to immobilize aptamer on the electrodes and strongly requires an additional material to help it form film, such as chitosan (CS). CS containing abundant amino groups with pK_a 6.3 is soluble in slightly acidic solution due to the protonation and insoluble in solution above pH 6.3 for the deprotonation, it exhibits robust film-forming ability. In addition, CS displays nontoxicity, biocompatibility, cheapness and a susceptibility to chemical modification. Because of its desirable properties, CS has been widely used as an immobilization matrix for biosensors and bioreactors.³²

Ferrocene (Fc) is attracting keen interest in the area of electroanalysis for the unique redox behavior. Because Fc is one of the most popular electrochemical active groups and the redox reaction of Fc^+/Fc is completely reversible, many scientists have used it in chemical modified electrodes.^{33–35} However, Fc can be poorly adsorbed onto the electrode surface. Thus, many materials had been used to improve the attachment of Fc and its derivatives to the electrode surface such as CS and MWCNTs.^{32,36} Due to their good properties *i.e.* high surface to volume ratio, and their chemical and thermal stability,³⁷ multi-walled carbon nanotubes (MWCNTs) exhibit a high ability to promote some types of electron-transfer reactions, minimize fouling of electrode surfaces, enhance electrocatalytic activity, and facilitate the immobilization of molecules such as enzymes or antibodies on their surface with a view to developing biosensors.³⁸ Recently, Zhou *et al.* has successfully synthesized multiwalled carbon nanotubes/ferrocene-branched chitosan composites and the sensor showed very good performance towards electrocatalytic determination of sulfite.³²

In the present work, a novel amperometric aptasensor was prepared by using mesoporous carbon (OMC) functionalized by chitosan (OMC-CS) and multiwalled carbon nanotubes/ferrocene-branched chitosan composites covered glassy carbon electrode. In this system, OMC functionalized with chitosan served as electronic bridge. The integration of CS-Fc and MWCNTs for the development of electrochemical aptasensor acted as signal amplifier, in addition, it also controlled the efficient immobilization of aptamers on the electrode. Based on the above mentioned advantages of these materials, we took advantage of their synergistic effects to fabricate a simple and sensitive aptasensor for detection of chlorpyrifos in real vegetable samples.

2. Experimental

2.1 Apparatus

Cyclic voltammetry (CV) measurements were performed with CHI660D electrochemical workstation (Shanghai Chenhua Co., China). A conventional three-electrode system was employed with a saturated calomel electrode (SCE) as the reference electrode, a platinum electrode as the auxiliary electrode, and a glassy carbon electrode (GCE) ($d = 3$ mm) or modified GCE as the working electrode. Scanning electron micrographs (SEM) was studied by JSM-6360LV SEM (Japan). An attached energy dispersive spectrometer (EDS) in the FE-SEM was applied to chemical composition analysis.

2.2 Reagents and materials

Chlorpyrifos was purchased from Sigma (USA). Bovine serum albumin (BSA) was from BioDev-Tech. Co. Ltd (Beijing, China). The chlorpyrifos oligonucleotides purchased from Shanghai Sangon Biological Engineering Technology & Services Co., Ltd. (Shanghai, China) with the following sequences:³⁹ 5-CCTGCC ACGCTCCGCAAGCTTAGGGTTACGCCTGCAGCGATTCTTGATC GCGCTGCTGGTAATCCTTCTTTAAGCTTGGCACCCGCATCGT-3'. Chitosan (CS) was purchased from Sangon Biotech Co., Ltd. (Shanghai, China). Ordered mesoporous carbons (OMC) which the external diameter is 3.9 nm was purchased from Nanjing Yoshikura nanotechnology co., LTD. Ferrocene (Fc) was purchased from Hongyan chemical reagent factory (Tianjin, China). 0.01 M phosphate buffer solution (PBS, pH 7.4, high-pressure sterilization) was used for dissolving the chlorpyrifos oligonucleotides. A PBS (0.1 M, pH 7.0) containing 5 mM $[Fe(CN)_6]^{3-/4-}$ and 0.1 M KCl was used as the detection solution. All of the other chemicals were analytical reagent grade. All the solutions were prepared with ultrapure water which was purified with a Milli-Q purification system (Branstead, USA).

2.3 Preparation of composites

Chitosan stock solution (CS) (0.20% (w/v)) was prepared by dissolving chitosan in an aqueous solution of 2.0 M acetic acid and the pH was adjusted to 5.0 by addition of concentrated NaOH solution. Then added 2 mg OMC into the CS solution and sonicating for 1 h to get 0.5 mg mL⁻¹ OMC-CS solution. The solution was stored in refrigerator.

Fc@MWCNTs composites were synthesized *via* a simple chemical strategy.⁴¹ Briefly, excessive Fc was added into 10 mL CS solution (pH = 5.0) to get the stable host–guest complexes by fully stirring. Then, 25 mg MWCNTs was dispersed into the 5 mL supernatant liquor and sonicated until it became stable dispersion. Therefore got Fc@MWCNTs-CS composites.

2.4 Fabrication of Fc@MWCNTs/OMC/GCE aptasensor

Procedure of the electrode preparation included five assemble processes, *i.e.* pretreatment of GCE, immobilization of OMC-CS, Fc@MWCNTs-CS, aptamer and BSA on the electrode surface (shown in Scheme 1). (1) GCE was polished successively with 1.0, 0.3, and 0.05 μm alumina powder, and sonicated in a 6.0 M nitric acid/ultrapure water and ethanol/ultrapure water for 20 min, respectively. Then, GCE as working electrode was subjected to cyclic scanning in 0.5 M H_2SO_4 solution in a potential range from -0.1 V to 1.0 V. When the cyclic voltammogram was almost unchanged, the electrode was taken out, cleaned with ultrapure water and dried under a stream of nitrogen. (2) A $7\ \mu\text{L}$ of the OMC-CS solution was coated onto the surface of the pretreated GCE using a microsyringe and dried at room temperature for over 2 h (denoted as OMC/GCE). (3) A $7\ \mu\text{L}$ of Fc@MWCNTs-CS solution was coated onto the surface of the OMC/GCE using a microsyringe and dried at room temperature (denoted as Fc@MWCNTs/OMC/GCE). (4) To immobilize the chlorpyrifos aptamer onto electrode interface, the electrode was immersed in chlorpyrifos aptamer solution at $4\ ^\circ\text{C}$ for about 12 h (denoted as Apt/Fc@MWCNTs/OMC/GCE). (5) Afterwards, the multilayer modified electrode was incubated with 0.5% BSA (denoted as BSA/Apt/Fc@MWCNTs/OMC/GCE) at $4\ ^\circ\text{C}$ for 2 h to eliminate nonspecific binding effect and block the remaining active groups, following by rinsing with PBS. The finished aptasensor was stored at $4\ ^\circ\text{C}$ when not in use.

2.5 Electrochemical detection of pesticides

All electrochemical measurements were performed in 0.1 M PBS (pH 7.0) containing 5 mM $\text{K}_3[\text{Fe}(\text{CN})_6]/\text{K}_4[\text{Fe}(\text{CN})_6]$ (1 : 1 mixture as a redox probe) and 0.1 M KCl. CVs were performed over a potential range from -0.2 to 0.6 V at a scan rate of $50\ \text{mV s}^{-1}$. The chlorpyrifos detection was based on change in the current response ($\Delta I(\Delta I = (I_0 - I_1))$), where I_0 is the peak current of the

CV after blocking nonspecific binding sites by BSA and I_1 is the peak current of the CV after chlorpyrifos coupling to the immobilized chlorpyrifos aptamer on the prepared aptasensor. In addition, the experimental parameters including aptamer concentration, incubation time and the pH of PBS were optimized. After the optimization, the proposed aptasensor was applied for detection of chlorpyrifos. All measurements were carried out at room temperature.

2.6 Preparation and determination of real samples

Fresh pakchoi, lettuce and leek bought from a local supermarket were washed, dried, chopped into $3 \times 3\ \text{mm}$ particles approximately. 10 g of each sample was sprayed with different concentrations of chlorpyrifos. After equilibration for 3 h at room temperature to make pesticide absorbed into the samples, 10 mL mixed solution of acetone and 0.1 M pH 7.5 phosphate buffer solutions (1/9, v/v) was added to the above samples. The suspensions were treated by ultrasonication for 15 min and then centrifuged for 10 min at 2000 rpm. The clear supernatant was analyzed for pesticide detection by employing the obtained aptasensor.

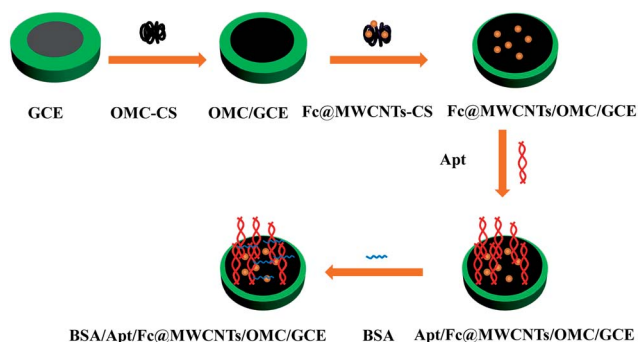
3. Results and discussion

3.1 SEM characterizations of modified electrodes

The morphologies of the OMC and Fc@MWCNTs composites were characterized using scanning electron microscope (SEM). As shown in Fig. 1(A), OMC nanofibers was distributed on the surface of GCE orderly and formed the current passages. Fig. 1(B) presented the SEM image of Fc@MWCNTs in $1\ \mu\text{m}$, and clearly illustrated a number of bright dots adulterate with the nanofibers, suggesting that the Fc had been dispersed into MWCNTs successfully. And Fig. 1(C) clearly revealed that Fe element distributed in the Fc@MWNTs. The SEM image of Fc@MWNTs/OMC as shown in Fig. 1(D), which illustrated that OMC was covered with Fc@MWNTs successfully.

3.2 Electrochemical behavior of the modified electrodes

The immobilisation of each functionalised layer on GCE surface was confirmed through CV measurements. Fig. 2 showed the cyclic voltammograms obtained for different modified electrodes in 0.1 M PBS (pH 7.0) containing 5 mM $\text{K}_3[\text{Fe}(\text{CN})_6]/\text{K}_4[\text{Fe}(\text{CN})_6]$ and 0.1 M KCl at the scan rate of $50\ \text{mV s}^{-1}$. There was a pair of well-defined redox peaks observed on the bare GCE with the anodic (E_{pa}) and cathodic (E_{pc}) peak potential of $0.26\ \text{V}$ and $0.15\ \text{V}$, respectively, and a peak to peak potential separation of about $95\ \text{mV}$ (Fig. 2(a)). The peak current increased after OMC-CS was modified on the surface of GCE (Fig. 2(b)), revealed that the OMC-CS film functioned as an electron-conducting tunnel. Furthermore, after coated with Fc@WMCNTs-CS, the peak current of obtained electrode further increased (Fig. 2(c)), indicated that the Fc@WMCNTs-CS film could promote the electron transfer between electrode surface and $[\text{Fe}(\text{CN})_6]^{3-/4-}$ and generate synergy on electrochemical properties. However, the redox peaks decreased obviously when aptamer (Fig. 2(d)) and BSA (Fig. 2(e)) were modified onto the electrode. It was reasonable that their



Scheme 1 Stepwise preparation of the aptasensor.

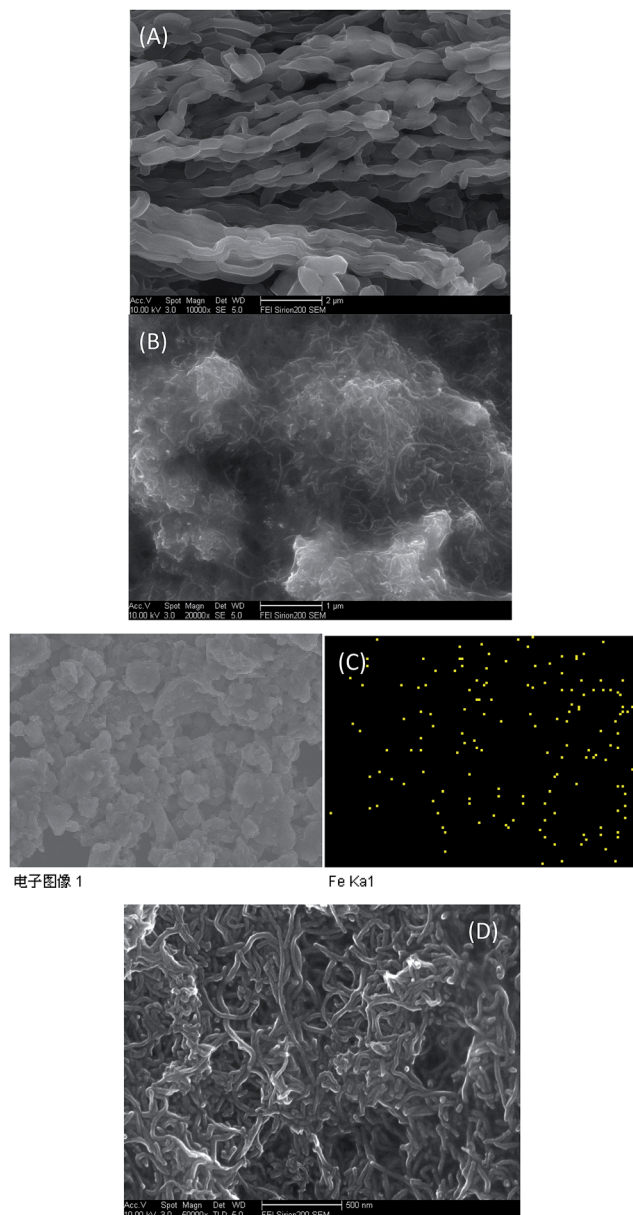


Fig. 1 SEM images of (A) OMC, (B) Fc-MWNTs, (D) Fc-MWNTs/OMC; (C) EDS for Fe elemental distribution on the surface of Fc@MWNTs.

non-electrochemical activity which partially blocked the electron transfer between the $[\text{Fe}(\text{CN})_6]^{3-/4-}$ solution and the electrode.

Fig. 3 shows the cyclic voltammograms of Apt/Fc@WMCNTs/OMC/GCE at different scan rates in potential range of 20–200 mV in 0.1 M PBS (pH 7.0). As shown in the inset of Fig. 3, the peak currents increased linearly with the scan rate between 20 and 200 mV s^{-1} as expected for a surface-controlled electrode process.⁴⁰

3.3 Optimization parameters of the biosensor performance

To achieve an optimal electrochemical signal, it was necessary to optimize the experimental conditions including the aptamer concentration, incubation time and pH of PBS. A

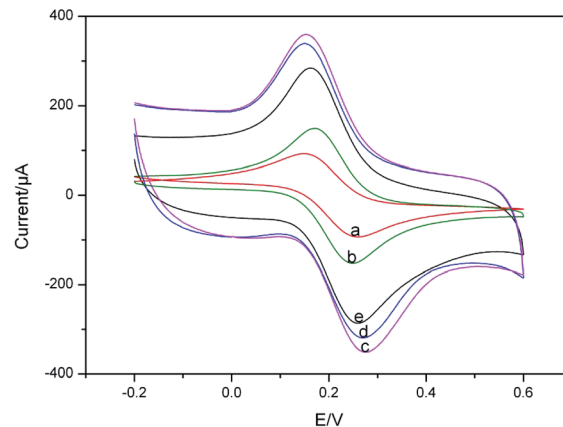


Fig. 2 CVs of modified GCE recorded in 0.1 M PBS (pH 7.0) containing 5.0 mM $[\text{Fe}(\text{CN})_6]^{3-/4-}$ and 0.1 M KCl: (a) bare GCE; (b) OMC/GCE; (c) Fc@MWCNTs/OMC/GCE; (d) Apt/Fc@MWCNTs/OMC/GCE; (e) BSA/Apt/Fc@MWCNTs/OMC/GCE.

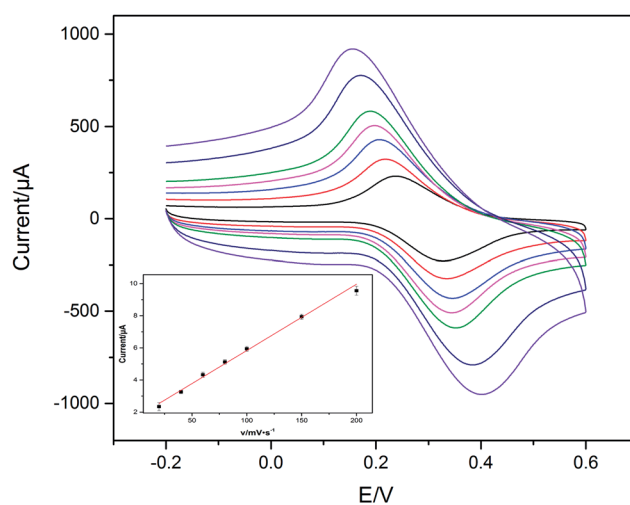


Fig. 3 Cyclic voltammograms of the Apt/Fc@WMCNTs/OMC/GCE in 0.1 M PBS (pH 7.0) at scan rates (from inner to outer) 20, 40, 60, 80, 100, 150 and 200 mV s^{-1} , respectively. Inset: the relationship between scan rates and peak currents.

series of aptamers with the concentrations from 1 to 10 μM were investigated to study the effect of the aptamer concentration. As displayed in Fig. 4(A), the change in current responses, was found to increase with the increasing of the aptamer concentration ranges from 1 to 2 μM and then decrease as the concentration increased further. The current responses reached the maximum at the aptamer concentration of 2 μM . The main reason is that for lower concentration of the aptamer the system becomes saturated and the affinitive reaction between chlorpyrifos and aptamer obeys the mass law.⁴² As a result, 2 μM chlorpyrifos aptamer was chosen for the subsequent assays.

Since it takes time for the chlorpyrifos immobilized on the electrode to react with the aptamer molecules to reach the saturated equilibrium, the effect of the incubation time was

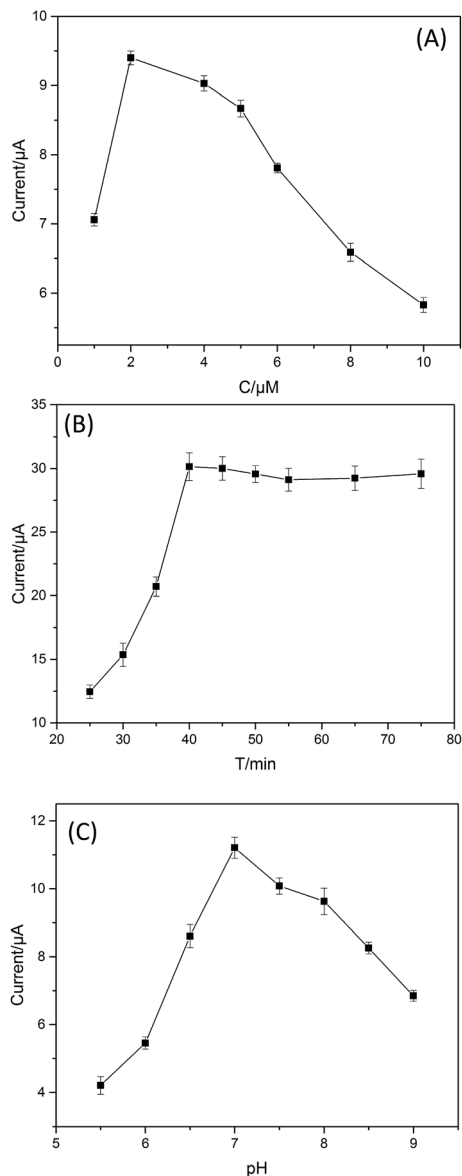


Fig. 4 (A) The optimum concentration of the aptamer; (B) the optimum incubation time; (C) the optimum pH of PBS.

carried out over the range of 25 to 85 min. As shown in Fig. 4(B), the current response reached the maximum in 40 min and remained stable when the time was extended, indicated that the interaction between aptamer and chlorpyrifos had reached saturation. Thus, 40 min was chosen as the adequate incubation time in all of the subsequent experiments.

In addition, the effect of pH on the sensor response was examined by recording CVs for the chlorpyrifos-captured electrode in 0.1 M PBS. The current increased as the medium pH was increased from 5.5 to 7.0 and then decreased when the pH value was higher than 7.0 (Fig. 4(C)). The maximum current was observed at a pH of 7.0. Therefore, all subsequent experiments were performed in 0.1 M PBS at pH 7.0.

3.4 Calibration curve of the aptasensor

On the basis of the optimal conditions, the proposed aptasensor was applied for chlorpyrifos detection. The CV current response (Fig. 5(A)) is linearly related to the logarithmic values of chlorpyrifos concentration range from 1 to 10^5 ng mL⁻¹ with a detection limit of 0.33 ng mL⁻¹ (S/N = 3). As Fig. 5(B) shown, the calibration plot shows a good linear relationship between CV current response and logarithmic values of chlorpyrifos concentration. The regression equation of the calibration curve was $Y = 20.921X + 6.175$ ($R^2 = 0.994$). The results demonstrated an acceptable quantitative performance of the proposed method used for chlorpyrifos detection.

3.5 Comparison of different methods

As shown in Table 1, a comparison of the designed aptasensor and other analytical methods. The detection limit of the designed aptasensor is significantly lower than other methods. The lower detection limit was attributed to the multiple amplified current of Fc@MWCNTs and OMC-CS.

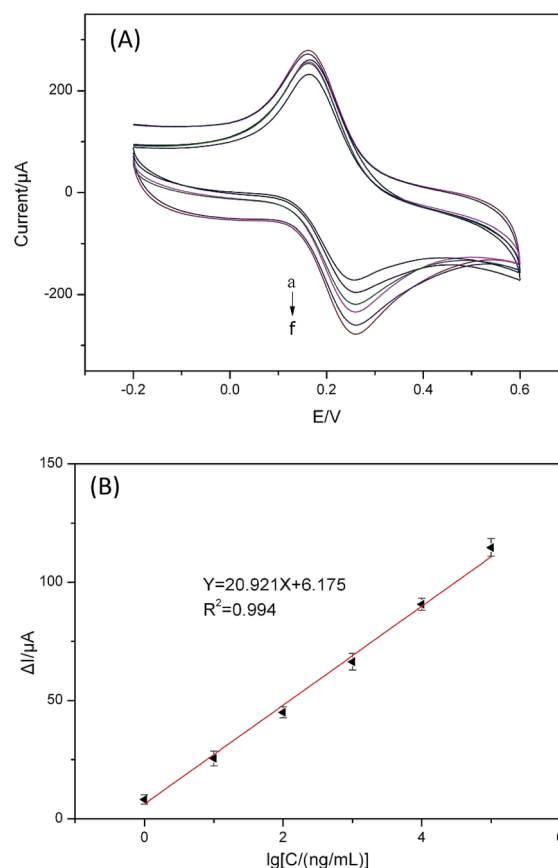


Fig. 5 The CVs (A) of the aptasensor after incubation in different concentrations of chlorpyrifos standard solution (from a to f): 10^5 , 10^4 , 1000, 100, 10, 1 ng mL⁻¹ under the optimal conditions; and the calibration curve (B) of the relative current changes (ΔI) of the proposed aptasensor versus the logarithm of chlorpyrifos concentrations.

Table 1 Comparison of analytical methods for the detection of pesticide

Analytical methods	Linear range (ng mL ⁻¹)	Detection limit (ng mL ⁻¹)	References
Fluorescence methods	578.325–7711	164.735	Azab <i>et al.</i> , 2015 (ref. 43)
CS-AuNPs-based colorimetric aptasensor	0.20–2.0	39	Luo <i>et al.</i> , 2015 (ref. 44)
Quantum dot–DNA aptamer conjugates coupled with capillary electrophoresis	112.1–3736.3	37.363–52.076	Tang <i>et al.</i> , 2016 (ref. 45)
Gas chromatography with flame photometric	4–1000	1–10	Zhao <i>et al.</i> , 2014 (ref. 46)
RAM-MIPs for selective solid-phase extraction	10–1000	0.5–1.9	He <i>et al.</i> , 2015 (ref. 47)
Aptasensor	1 to 1 × 10 ⁵	0.33	This work

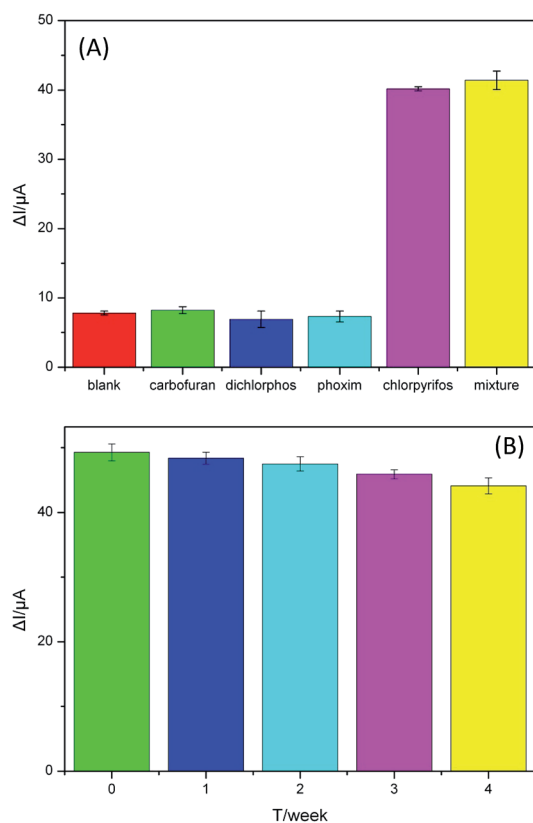


Fig. 6 (A) Selectivity evaluation of the aptasensor detection of chlorpyrifos (50 ng mL⁻¹) against the interference molecules, carbofuran, dichlorphos, phoxim and the mixture consisting of the above interference and chlorpyrifos. (B) The stability assessment of the proposed aptasensor.

3.6 Selectivity, reproducibility and stability of the aptasensor

To investigate the selectivity of the aptasensor, we detected the current response of the aptasensor to chlorpyrifos, other small molecules (carbofuran, dichlorphos, phoxim) commonly present in real samples with same concentration of 50 ng mL⁻¹ and their mixture. As seen from Fig. 6(A), no apparent changes in the current are observed toward these components, indicating the high selectivity of the developed aptasensor for chlorpyrifos detection.

The reproducibility of the aptasensor, an important parameter, was investigated by determining 50 ng mL⁻¹ chlorpyrifos

Table 2 The recovery of the proposed aptasensor in real samples

Sample	Original vegetable	Added (ng mL ⁻¹)	Totally found (ng mL ⁻¹)	Recovery (%)
Leek	No found	10	10.72	107.2
Lettuce	—	5	5.16	103.2
Pakchoi	—	10	9.85	98.5

solution with six electrodes fabricated in the same conditions. The relative standard deviation (RSD) of the measurements for the six electrodes was 4.3%, which indicated that the aptasensor has good reproducibility.

The stability of the proposed aptasensor is evaluated by successive cyclic scans for 30 cycles and long-term storage assay. After 30 cycles' continuous CV measurements under the optimal conditions, a 4.8% decrease of the initial signal is found. In addition, the storage stability of the proposed aptasensor was evaluated by storing the aptasensors prepared under the same conditions at 4 °C and measuring every week, and each reading represented the average value of five assays. After 2 week, the current response of the aptasensor had little change, only 3.6% (Fig. 6(B)). The initial current response was not found to be significantly changed for 4 weeks and the aptasensor could remain about 89.3% of the initial response. Thus, the aptasensor has acceptable storage stability.

3.7 The detection of the real samples

To evaluate the practical application and potential prospects of the proposed aptasensor, recovery experiments were performed by standard addition methods in vegetable samples. The experiments were carried out according to the aforementioned optimized conditions for chlorpyrifos detection by the designed aptamer sensor. The chlorpyrifos concentration recoveries were between 98.5% and 107.2% (Table 2), which clearly indicated that the aptasensor was suitable for the detection of chlorpyrifos in real vegetable samples.

4. Conclusions

In summary, a sensitive electrochemical aptasensor based on OMC-CS and Fc@WMCNTs-CS double-assisted signal amplification was proposed for chlorpyrifos detection. The designed

aptasensor exhibited a linear response with a wide range (1 to 10^5 ng mL⁻¹), low detection limit (0.33 ng mL⁻¹) and high levels of specificity, reproducibility and stability. In addition, the aptasensor has been applied to detect chlorpyrifos in real samples, and got a satisfactory results. Therefore, the designed aptasensor may hold great potential applications for food analysis.

Acknowledgements

This work was supported by the National Natural Science Foundation of China (No. 30972055, 31101286, 31471641), Agricultural Science and Technology Achievements Transformation Fund Projects of the Ministry of Science and Technology of China (No. 2011 GB2C60020), Special project of independent innovation of Shandong Province (2014CGZH0703) and Shandong Provincial Natural Science Foundation, China (No. Q2008D03, ZR2014CM009, ZR2014FL003, ZR2015CM016). Science and technology project of Shandong Province, China (No. J11LD23).

References

- 1 A. T. Farag, A. M. Okazy and A. F. Aswed, *Reprod. Toxicol.*, 2003, **17**, 203–208.
- 2 H. Tian, Z. T. Zheng, J. G. Li and G. B. Ye, *Agrochemicals*, 2014, **53**, 832–835.
- 3 G. F. Qin, Y. B. Li, Y. Chen, Q. Y. Sun, B. Zuo, F. R. He, N. M. Shen, G. F. Jia and G. R. Ding, *Food Res. Int.*, 2015, **72**, 161–167.
- 4 M. A. Z. Chowdhury, A. N. M. Fakhruddin, M. N. Islam, M. Moniruzzaman, S. H. Gan and M. K. Alam, *Food Control*, 2013, **34**, 457–465.
- 5 H. X. Guan, W. E. Brewer, S. T. Garriss and S. L. Morgan, *J. Chromatogr. A*, 2010, **1217**, 1867–1874.
- 6 A. Heccegova, M. Dömötöro and E. Matisova, *J. Chromatogr. A*, 2007, **1153**, 54–73.
- 7 S. Mostafalou and M. Abdollahi, *Toxicol. Appl. Pharmacol.*, 2013, **268**, 157–177.
- 8 S. Y. Liu, Z. T. Zheng, F. L. Wei, Y. P. Ren, W. J. Gui, H. M. Wu and G. N. Zhu, *J. Agric. Food Chem.*, 2010, **58**, 3271–3278.
- 9 S. Seccia, P. Fidente, D. Montesano and P. Morrica, *J. Chromatogr. A*, 2008, **1214**, 115–120.
- 10 W. Xie, C. Han, Y. Qian, H. Y. Ding, X. M. Chen and J. Y. Xi, *J. Chromatogr. A*, 2011, **1218**, 4426–4433.
- 11 B. H. Zhang, X. P. Pan, L. Venne, S. Dunnum, S. T. Mcmurry, G. P. Cobb and T. A. Anderson, *Talanta*, 2008, **75**, 1055–1060.
- 12 X. A. Zhang, N. Mobley, J. G. Zang, X. M. Zheng, L. Lu, O. Ragin and C. J. Smith, *J. Agric. Food Chem.*, 2010, **58**, 11553–11556.
- 13 H. J. Kim, W. L. Shelver and Q. X. Li, *Anal. Chim. Acta*, 2004, **509**, 111–118.
- 14 H. Y. Zhao, X. P. Ji, B. B. Wang, N. Wang, X. R. Li, R. X. Ni and J. J. Ren, *Biosens. Bioelectron.*, 2015, **65**, 23–30.
- 15 Y. Li, Y. Bai, G. Han and M. Li, *Sens. Actuators, B*, 2013, **185**, 706–712.
- 16 Q. Zhou, L. Yang, G. Wang and Y. Yang, *Biosens. Bioelectron.*, 2013, **49**, 25–31.
- 17 L. Liu, D. Xu, Y. Y. Hu, S. Z. Liu, H. L. Wei, J. G. Zheng, G. X. Wang, X. Y. Hu and C. Y. Wang, *Food Control*, 2015, **53**, 72–80.
- 18 J. M. Song, M. Culha, P. M. Kasili, G. D. Griffin and T. Vo-Dinh, *Biosens. Bioelectron.*, 2005, **20**, 2203–2209.
- 19 Z. Wu, J. Li, M. Luo, G. Shen and R. Yu, *Anal. Chim. Acta*, 2005, **528**, 235–242.
- 20 M. Citartan, S. C. B. Gopinath, J. J. Tominaga, S. C. Tan and T. H. Tang, *Biosens. Bioelectron.*, 2012, **34**, 1–11.
- 21 Y. S. Kim, N. H. A. Raston and M. B. Gu, *Biosens. Bioelectron.*, 2016, **76**, 2–19.
- 22 S. D. Jayasena, *Clin. Chem.*, 1999, **45**, 1628–1650.
- 23 J. A. Hansen, J. Wang, A. N. Kawde, Y. Xiang, K. V. Gothelf and G. Collins, *J. Am. Chem. Soc.*, 2006, **128**, 2228–2229.
- 24 X. Sun, F. L. Li, G. H. Shen, J. D. Huang and X. Y. Wang, *Analyst*, 2014, **139**, 299–308.
- 25 Y. Zhu, J. I. Son and Y. B. Shim, *Biosens. Bioelectron.*, 2010, **26**, 1002–1008.
- 26 S. J. Guo, Y. Du, X. Yang, S. J. Dong and E. K. Wang, *Anal. Chem.*, 2011, **83**, 8035–8040.
- 27 S. B. Xie, Y. Q. Chai, Y. L. Yuan, L. J. Bai and R. Yuan, *Biosens. Bioelectron.*, 2014, **55**, 324–329.
- 28 R. Ryoo, S. H. Joo and S. Jun, *J. Phys. Chem. B*, 1999, **103**, 7743–7746.
- 29 Z. Zhou and M. Hartmann, *Chem. Soc. Rev.*, 2013, **42**, 3894–3912.
- 30 Y. Y. Zhou, L. Tang, G. M. Zeng, C. Zhang, X. Xie, Y. Y. Liu, J. J. Wang, J. Tang, Y. Zhang and Y. C. Deng, *Talanta*, 2016, **146**, 641–647.
- 31 H. Werner, *Angew. Chem., Int. Ed.*, 2012, **51**, 6052–6058.
- 32 H. Zhou, W. W. Yang and C. Q. Sun, *Talanta*, 2008, **77**, 366–371.
- 33 V. S. Elanchezhian and M. Kandaswarny, *Inorg. Chem. Commun.*, 2009, **12**, 161–165.
- 34 J. D. Qiu, W. M. Zhou, J. Guo, R. Wang and R. P. Liang, *Anal. Biochem.*, 2009, **385**, 264–269.
- 35 J. B. Raoof, R. Ojani and M. Kolbadinezhad, *J. Solid State Electrochem.*, 2009, **13**, 1411–1416.
- 36 G. C. Zhao, M. Q. Xu and Q. Zhang, *Electrochem. Commun.*, 2008, **10**, 1924–1926.
- 37 A. Fatoni, A. Numnuam, P. Kanatharana, W. Limbut, C. Thammakhet and P. Thavarungkul, *Sens. Actuators, B*, 2013, **185**, 725–734.
- 38 M. Valcárcel, S. Cárdenas and B. M. Simonet, *Anal. Chem.*, 2007, **79**, 4788.
- 39 Z. J. Lei, C. Z. Zhang, Y. Liu, L. Wang, Q. H. Hu and X. J. Liu, *Jiangsu J. of Agr. Sci.*, 2012, **28**, 198–203.
- 40 D. X. Xie, Y. N. Mao and J. G. Ma, *Funct. Mater.*, 2010, **41**, 57–59.
- 41 G. D. Liu and Y. H. Lin, *Electrochem. Commun.*, 2005, **7**, 339–343.
- 42 L. Qiao, Y. M. Guo, X. Sun, Y. C. Jiao and X. Y. Wang, *Bioprocess Biosyst. Eng.*, 2015, **38**, 1455–1468.
- 43 H. A. Azab, Z. M. Anwar, M. A. Rizk, G. M. Khairy and M. H. El-Asfoury, *J. Lumin.*, 2015, **157**, 371–382.

- 44 Y. L. Luo, J. Y. Xu, Y. Li, H. T. Gao, J. J. Guo, F. Shen and C. Y. Sun, *Food Control*, 2015, **54**, 7–15.
- 45 T. T. Tang, J. J. Deng, M. Zhang, G. Y. Shi and T. S. Zhou, *Talanta*, 2016, **146**, 55–61.
- 46 X. S. Zhao, W. J. Kong, J. H. Wei and M. H. Yang, *Food Chem.*, 2014, **162**, 270–276.
- 47 J. He, L. X. Song, S. Chen, Y. Y. Li, H. L. Wei, D. X. Zhao, K. R. Gu and S. S. Zhang, *Food Chem.*, 2015, **187**, 331–337.